Journal of Materials Chemistry C

Accepted Manuscript

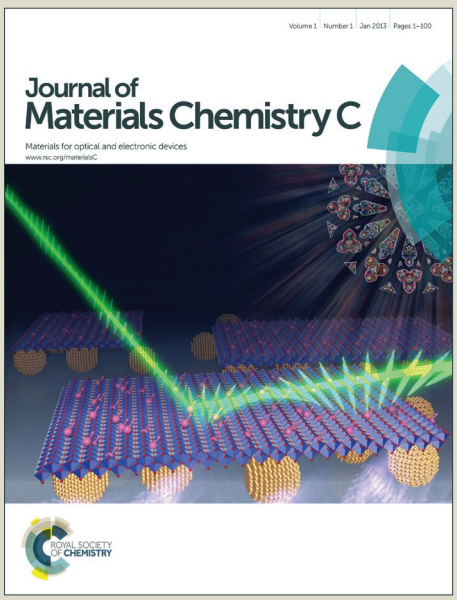

ROYAL SOCIETY OF CHEMISTRY

www.rsc.org/materialsC

Journal of Materials Chemistry C RSCPublishing

ARTICLE

Circularly polarized light emission from chiral nematic phenylterthiophene dimer exhibiting ambipolar carrier transport

Taichi Hamamoto and Masahiro Funahashi

siCite this: DOI: 10.1039/x0xx00000x

Received ooth January 2012,
Accepted ooth January 2012

DOI: 10.1039/x0xx00000x

www.rsc.org/

A dimer bearing two phenylterthiophene parts linked by a chiral moiety with a minimized molecular volume has been synthesized. This chiral dimer exhibits a chiral nematic phase and its helical structure can be fixed by cooling rapidly. The helical pitch is shorter than the visible light wavelength and the reflection band can be tuned between near ultraviolet and infrared wavelength by mixing enantiomers of the dimer or changing the temperature. The hole and electron mobilities in the chiral nematic phase are of the order of 10^{-5} $cm^2V^{-1}s^{-1}$. Circularly polarized light emission has been observed in the chiral nematic phase. In fluidic chiral nematic phase, circularly polarized photoluminescence can be switched to non-polarized state reversibly by the application of the electric field.

Introduction

Supramolecular self-assemblies to organize π-conjugated moieties are promising optoelectronic materials. Electronic carrier transport has been observed in the columnar[2] and smectic phases.[3] Solution-processable liquid-crystalline (LC) semiconductors have been applied to field-effect transistors,[4] polarized electroluminescence devices,[5] and solar cells.[6]

Unlike crystals, LC phases are characterized by their dynamic nature. Therefore new optical and electronic functions which are tunable by external stimuli can be created by the construction of dynamic superstructures in the LC phases.[7] One method is the formation of nanostructures through nanosegregation of LC molecules consisting of incompatible parts.[8a-c] Electrochromism was observed in the nanosegregated smectic phases[8d-e] and efficient electron transport was reported in nanosegregated columnar phases of LC materials bearing oligosiloxane moieties.[9]

Chirality is also another key to construct supramolecular nanostructures in the LC systems. Chiral LC molecules can form fascinating superstructures with optical or electronic functions, such as chiral nematic,[10] chiral smectic C,[11] twisted grain boundary,[12] and blue phase LCs.[13] Chiral nematic LC materials form one-dimensional photonic stop band in the range of visible light wavelength.[10] Circularly polarized luminescence (CPL)[14] and laser emission[15] have been observed from chiral nematic LCs. Only optically pumped systems have been previously reported, in which luminescent dye molecules are dispersed in electronically inactive chiral nematic LCs.[14c-e,15]

For electrically pumped systems, high density of the chromophores is requisite. However, nematic and chiral nematic LCs are generally unfavorable for electronic carrier transports in contrast to columnar[2] and smectic LC phases.[3] Since the experiments of photoconductive nematic LCs by Yoshino[16a] and Kusabayashi,[16b] ionic conduction has been predominant in the nematic and chiral nematic phases.[16]

In the last decade, electronic charge carrier transport has been confirmed in the nematic and chiral nematic LCs having extended π-conjugated chromophores.[17] For CPL emission, helical pitches of chiral nematic LCs are comparable with the visible light wavelength. It is noted that CPL emission is obtained only within the reflection band of a chiral nematic phase. The extended π-conjugated cores are effective to expand the width of the reflection band, due to the large anisotropy in the refractive index. Woon *et al*. obtained CPL emission in the range of visible light wavelength over 100 nm, using a hole transporting chiral nematic LC having long chiral alkyl chains.[18a] Its circular dissymmetry factor (g_e) was extremely high. However, the reflection band of the chiral nematic LC was fixed in blue and yellow region and the reflection band was not tunable.

Chiral nematic LCs bearing a binaphthyl spacer have been used for chiral dopant and reaction media.[10e] We reported phenylquaterthiophene dimers bearing a binaphthyl group as a chiral spacer.[18b] The helical twisting power is so strong that the reflection band can be tuned between near UV and near IR wavelength by mixing it with achiral LCs or changing the temperature. However, the bulky binaphthyl group is electronically inactive, resulting in low carrier mobility. A

chiral moiety to exhibit a strong helical twisting power with a minimized free volume is indispensable for CPL emission from electrically pumped chiral nematic LC systems.

Herein we report a dimeric chiral LC molecule bearing a minimized chiral moiety and extended π-conjugated systems which act as a hopping site of charge carriers as well as a luminescent chromophore. The value of g_e reaches 1.5 at the maximum. It should be noted that the helical twisting power of the chiral nematic compound is sufficiently strong and the reflection band is tunable between UV and near IR regions. Moreover, the colour of the fluorescence can be changed by the application of DC bias in the fluidic chiral nematic phase of the compound.

Moreover, this compound exhibits ambipolar charge carrier transport in the chiral nematic phase. Elongation of the π-conjugated systems is effective to increase the carrier mobility and the birefringence of the LC materials, resulting in expansion of the reflection band. However, excessive extension of the π-conjugated systems leads to red-shift of absorption band. In this study, phenylterthiophene core is adopted as a luminescent chromophore.

The helical structure of the chiral nematic phase of the dimeric LC compound can be fixed in the glassy phase by the rapid cooling. Dimeric compounds consisting of two cholesteryl groups and alkyl or diacetylene spacers exhibit a glassy chiral nematic phase at room temperature and can form thin films exhibiting selective reflections for visible light.[10]

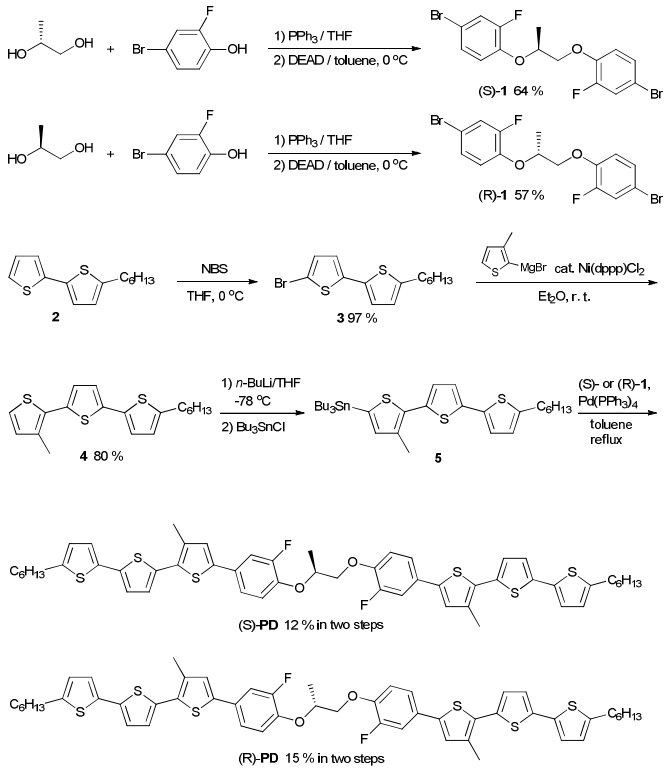

Scheme 1 Synthetic route toward (S)- and (R)-1,2-Bis[4-(5-hexyl-3''-methyl-2,2':5',2''-terthien-5''-yl)-2-fluorophenoxy]propane ((S)-**PD,** (R)-**PD**).

Experimental methods

The phase transition behaviour was characterized by polarizing optical microscopy, differential scanning calorimetry (DSC), and Cu Kα_1 X-ray diffraction (XRD). An optical texture of a chiral nematic phase was observed under a polarized light microscope Olympus DP70 equipped with a hand-made hot stage. The phase transition temperature and the transition enthalpy were determined with a NETZSCH Maia DSC 200 F3. The positional ordering of the chiral nematic molecules were measured by a diffractometer Rigaku Rapid II.

The carrier mobilities were determined by a time-of-flight (TOF) method[19] under atmospheric conditions. The isotropic chiral dimer was capillary-filled into LC cell consisted of two ITO-coated glass plates on a hot stage. DC voltage was applied to the LC cells by an electrometer (ADC R8252), and a Nd: YAG pulse laser (Continuum MiniLite II) was illuminated on one side of it. The chiral nematic compound exhibited a strong absorption band around 400 nm and the penetration depth of the laser pulse (wavelength = 356 nm) was much shorter than the sample thickness. For this reason, a sheet of photocarriers was generated near the illuminated electrode. The photocarriers drifted across the bulk of the sample under the electric field, and the induced displacement current was recorded as a voltage drop through a serial resistor by a digital oscilloscope (Tektronics TDS 3044B). The displacement current was constant while the charge carriers drifting, and decreased to zero when they arrived at the counter electrode. The transit time t_T was determined from the kink points of the transient photocurrent curves. The carrier mobility μ was calculated from equation 1, where d is the cell thickness and V is the applied voltage.

$$\mu = \frac{d^2}{V t_T} \qquad (1)$$

The electrode surface was not treated in the experiments. From the observation of the polarizing optical micrographic textures, the LC molecules form helical structures of which the directions of helical axes are random during the application of DC voltage in the experiments.

Photonic bands of the LC samples were examined by transmittance and circularly polarized photoluminescence spectra. Transmittance spectra measurements were conducted on a Jasco V-530 spectrophotometer to determine absorption and stop bands of the glassy chiral nematic films cooled rapidly from 106 ºC or 95 ºC. Circularly polarized photoluminescence spectra were measured using an Ocean Optics spectrometer equipped with $\lambda/2$ and $\lambda/4$ filters. The handedness of the CPL luminescence is determined by the order of the two filters. For the optical measurements, a mechanically-rubbed polyimide (PI) alignment layer was prepared on a glass substrate. Butyl

cellosolve solutions of PI varnish (SE-150 (0821)) and thinner (26 Thinner) supplied from Nissan Chemical Industries, Ltd., were mixed at a ratio of 1:2 for PI solution and thinner solution, respectively. The mixture was spun on a glass plate at increasing rates of 500 rpm for 10sec., 1500 rpm for 10 sec., and 3000 rpm for 20 sec. The glass plate were annealed in an oven for 3 hours at 200 ºC and the surfaces of the PI thin films deposited on the glass plates were rubbed along the longitudal direction of the substrates.

Material Synthesis

The chiral dimer in this study bears two phenyltertionphene parts and one (S)-propane moiety as shown in Scheme 1.[20] It was synthesized by a Pd(0)-catalyzed Stille coupling between 5-tributylstannyl-5''-hexyl-3-methyl-2,2':5',2''-terthiophene and (S)-1,2-di(4-bromo-2-fluorophenoxy)-propane. (R)-(-)-1,2-propanediol, 4-bromo-2-fluorophenol, 5-hexyl-2,2'-bithiophene and 2-bromo-3-methylthiophene were commercially available from Aldrich. Silica gel was purchased from Kanto Chemicals. All purchased materials were used as received. ^{1}H and ^{13}C nuclear magnetic resonance (NMR) spectra were recorded on a Varian UNITY INOVA 400NB spectrometer. Fourier transform infrared (FT/IR) spectra were determined using JASCO FT/IR-660 Plus. Mass spectra measurements were conducted on a BRUKER ultraflextreme.

(S)-1,2-di(4-bromo-2-fluorophenoxy)-propane. ((S)-1)

A solution of diethyl azodicarboxylate (DEAD) in toluene (60 ml, 132 mmol) was added dropwise to a dry THF solution (150 ml) of (R)-(-)-1,2-Propanediol (5g, 66 mmol), 4-Bromo-2-fluoro-phenol (25.21 g, 132 mmol) and triphenylphosphine (34.58 g, 132 mmol) at 0 ºC. After stirring for 5 hours, the reaction solution was quenched with aqueous NaOH (100 ml) and extracted with ethyl acetate. The extract was dried over Na_2SO_4, filtered and concentrated in vacuo. Precipitated phosphine oxide was filtered off and washed with *n*-hexane several times. The filtrate was concentrated onto a silica gel for purification by a flash column chromatography (the eluant was *n*-hexane) and recrystallization from *n*-hexane to yield colorless powders (17.77 g, 64 %).
^{1}H NMR (400MHz, $CDCl_3$) δ = 1.43 (3H, d, J = 6.4 Hz), 4.07 (1H, dd, J = 4.0 Hz), 4.18 (1H, dd, J = 6.4 Hz), 4.66 (1H, sextet, J = 5.6 Hz), 6.85 (1H, t, J = 8.8 Hz), 6.96 (1H, t, J = 8.8 Hz), 7.16 (2H, d, J = 8.4 Hz), 7.24(2H, d, J = 8.4 Hz). IR (ATR) 574, 637, 767, 800, 860, 880, 1040, 1124, 1207, 1269, 1310, 1376, 1410, 1453, 1491, 1590, 2942, 2988, 3081cm^{-1}. Exact mass: 418.91. Molecular weight: 421.05. Mass (MALDI-TOF) Found: m/z (MNa^+): 441.82, 443.44, 444.43, 445.43, 446.43, 447.43. Calculated: m/z: 420.91, 418.91, 422.91, 421.91, 419.91, 423.91. Elemental analysis calcd (%): C, 42.79; H, 2.63; Br, 37.95; F, 9.02; O, 7.60.; found: C, 42.8; H, 2.9.

(R)-1,2-di(4-bromo-2-fluorophenoxy)-propane. ((R)-1)

A solution of diethyl azodicarboxylate (DEAD) in toluene (60 ml, 132 mmol) was added dropwise to a dry THF solution (150 ml) of (R)-(-)-1,2-Propanediol (5.0 g, 66 mmol), 4-Bromo-2-fluoro-phenol (25.10 g, 132 mmol) and triphenylphosphine (34.5 g, 132 mmol) at 0 ºC. After stirring for 5 hours, the reaction solution was quenched with aqueous NaOH (100 ml) and extracted with ethyl acetate. The extract was dried over Na_2SO_4, filtered and concentrated in vacuo. Precipitated phosphine oxide was filtered off and washed with *n*-hexane several times. The filtrate was concentrated onto a silica gel for purification by a flash column chromatography (the eluant was *n*-hexane) and recrystallization from *n*-hexane to yield colorless powders (15.9 g, 57 %).
^{1}H NMR (400MHz, $CDCl_3$) δ = 1.43 (3H, d, J = 6.4 Hz), 4.07 (1H, dd, J = 4.0 Hz), 4.18 (1H, dd, J = 6.4 Hz), 4.66 (1H, sextet, J = 5.6 Hz), 6.85 (1H, t, J = 8.8 Hz), 6.96 (1H, t, J = 8.8 Hz), 7.16 (2H, d, J = 8.4 Hz), 7.24(2H, d, J = 8.4 Hz). IR (ATR) 574, 637, 767, 800, 860, 880, 1040, 1124, 1207, 1269, 1310, 1376, 1410, 1453, 1491, 1590, 2942, 2988, 3081cm^{-1}. Elemental analysis calcd (%): C, 42.79; H, 2.63; Br, 37.95; F, 9.02; O, 7.60.; found: C, 42.6; H, 2.7.

5'-Bromo-5-hexyl-2,2'-bithiophene. (3)

N-bromosuccinimide (3.53 g, 20 mmol) was added to a stirred solution of 5-hexyl-2,2'-bithiophene (5 g, 20 mmol) in dry THF (50 ml) at 0 ºC and the temperature was allowed to warm to room temperature. After stirring for 3 hours, the reaction mixture was quenched with aqueous Na_2CO_3 (50 ml) and extracted with *n*-hexane. The extract was dried over Na_2SO_4, filtered and concentrated in vacuo. The crude product was purified by a flash column chromatography (silica gel, the eluant was *n*-hexane) and recrystallization from *n*-hexane to yield colourless powders (6.04 g, 97 %). This compound contained some amount of impurity, but it was used for the next reaction step without further purification.
^{1}H NMR (400 MHz, $CDCl_3$) δ = 0.88 (3H, t, J = 6.0 Hz), 1.30 (4H, m), 1.36 (2H, quint, J = 4.4 Hz), 1.66 (2H, quint, J = 7.2 Hz), 2.77 (2H, t, J = 7.6 Hz), 6.65 (1H, d, J = 2.4 Hz), 6.82 (1H, d, J = 3.6 Hz), 6.90 (1H, d, J = 2.8 Hz), 6.93 (1H, d, J = 3.2 Hz). Exact mass: 328.00. Molecular weight: 329.32. Mass (MALDI-TOF) Found: m/z (M^+): 327.42, 328.41, 329.42, 330.42, 331.43. Calculated: m/z: 329.99, 328.00, 331.00, 330.99, 328.99, 332.99, 332.00, 330.00.

5-Hexyl-3''-metyl-2,2':5',2"-terthiophene. (4)

2-Bromo-3-methylthiophene (3.25 g, 18.2 mmol) was slowly added dropwise to a stirred dispersion of magnesium (531.8 mg, 21.8 mmol) and a single grain of iodine in dry diethyl ether (60 ml). After the exothermal reaction was completed, 1,2-dibromoethane (0.3 ml) was added to reaction mixture in order to quench unreacted magnesium. After stirring for 2 hours, [1,3-bis(diphenylphosphino)propane]-dichloro-nickel (II) (20 mg, 37 μmol) and compound **3** (3.25 g, 9.12 mmol) were added to the reaction mixture, which was then stirred for 5 hours at 0 ºC. The reaction mixture was quenched by pouring into aqueous ammonium chloride solution (300 ml), extracted with *n*-hexane/ ethyl acetate (10:1). The extract was dried over Na_2SO_4, filtered and concentrated in vacuo. The crude product

was purified by a flash column chromatography (silica gel, the elutant was *n*-hexane) and crystallization from *n*-hexane to yield yellow crystals (2.53 g, 80 %).

^{1}H NMR (400MHz, $CDCl_3$) δ = 0.88 (3H, t, J = 6.8 Hz), 1.30 (4H, m), 1.36 (2H, quint, J = 6.5 Hz), 1.66 (2H, quint, J = 7.5 Hz), 2.39 (3H, s), 2.77 (2H, t, J = 7.6 Hz), 6.67 (1H, d, J = 3.3 Hz), 6.86 (1H, d, J = 5.2 Hz), 6.97 (1H, d, J = 3.5 Hz), 6.99 (1H, d, J = 3.7 Hz), 7.02 (1H, d, J = 3.9 Hz), 7.11 (1H , d, J = 5.1 Hz). IR (ATR) 789, 831, 857, 1065, 1455, 2857, 2924, 2963, 3079, 3103 cm^{-1}. Exact mass: 346.09. Molecular weight: 346.57. Mass (MALDI-TOF) Found: m/z (M^+): 345.56, 346.53, 347.54, 348.54, 349.57. Calculated: m/z: 346.09, 347.09, 348.08, 349.09, 348.10. Elemental analysis calcd (%): C, 65.85; H, 6.40; S, 27.76.; found: C, 65.55; H, 6.44.

5-Tributylstannyl-5''-hexyl-3-methyl-2,2':5',2''-terthiophene. (5)

n-BuLi (10.6 ml, 17.0 mmol) were slowly added dropwise to a stirred solution of compound **4** (4.5 g, 15.5 mmol) in dry THF (110 ml) at -78 ºC. The mixture was allowed to come to room temperature and stirred for 30 minutes. Tributyltin chloride (5.29, 16.3 mmol) was added dropwise at -78 ºC to the solution, which was then stirred for 3 hours at room temperature. The reaction mixture was quenched with aqueous NH_4Cl solution and extracted with *n*-hexane. The extract was dried over Na_2SO_4 and filtrated. After the solvent was evaporated, yellow oily product (8.98g) was obtained and used for next reaction without further purification.

^{1}H NMR (400MHz, $CDCl_3$) δ = 0.90 (12H, t, J = 7.2 Hz), 1.34 (12H, m), 1.58 (8H, sextet, J = 8.4 Hz), 1.67 (6H, quint, J = 7.2 Hz), 2.42 (3H, s), 2.78 (2H, t, J = 7.2 Hz), 6.67 (1H, d, J = 3.6 Hz), 6.91 (1H, s), 6.97 (1H, d, J = 3.6 Hz), 6.99 (1H, d, J = 3.6 Hz), 7.02 (1H, d, J = 3.6 Hz)

(S)-1,2-Bis[4-(5-hexly-3''-methyl-2,2':5',2"-terthien-5''-yl)-2-fluorophenoxy]propane. ((S)-PD)

A mixture of compound **1** (3 g, 3.7 mmol), compound **5** (4.73 g, 7.4 mmol) and tetrakis(triphenylphosphine)palladium(0) (300 mg, 0.26 mmol) in toluene (150 ml) was refluxed for 12 hours and cooled to room temperature. The reaction mixture was stirred with aqueous KF (10 wt%, 100 ml) for 30 minutes and extracted with toluene. The extract was dried over Na_2SO_4, filtered and concentrated in vacuo. The crude product was purified by a silica gel flash column chromatography (the eluant was hot cyclohexane : toluene = 2 : 1 and hot cyclohexane : THF = 1 : 5). The crude crystals were recrystallized from toluene several times to obtain (S)-**PD** as pale yellow crystals (0.84 g, 12 % in two steps).

^{1}H NMR (400MHz, $CDCl_3$) δ = 0.88 (6H, t, J = 6.8 Hz) , 1.30 (9H, d, J = 6.4 Hz) , 1.37 (4H, quint, J = 8.8 Hz) , 1.48 (3H, d, J = 6.0 Hz) , 1.66 (4H, quint, J = 7.6 Hz) , 2.39 (6H, s) , 4.13 (1H, dd, J = 4.4 Hz), 4.27 (1H, dd, J = 5.6 Hz), 4.75 (1H, sextet, J = 5.6 Hz) 6.67 (2H, d, J = 2.8 Hz), 6.96 (1H, t, J = 8.4 Hz) , 6.97 – 7.04 (8H, m) , 7.08 (1H, t, J = 8.4 Hz) , 7.22 – 7.31 (4H, m) IR (ATR) 792, 881, 958, 1002, 1128, 1227, 1299, 1302, 1370, 1459, 1508, 1629, 2851, 2928, 2964 cm^{-1}. Exact mass: 952.24. Molecular weight: 953.38. Mass (MALDI-TOF) Found: m/z (M^+): 952.29, 953.31, 954.31, 955.31, 956.31, 957.31. Calculated: m/z: 952.24, 953.24, 954.24, 954.25, 955.24, 956.24, 955.25, 956.23. Elemental analysis calcd (%): C, 66.77; H, 5.71; F, 3.99; O, 3.36; S, 20.18.; found: C, 66.8; H, 5.7.

(R)-1,2-Bis[4-(5-hexly-3''-methyl-2,2':5',2"-terthien-5''-yl)-2-fluorophenoxy]propane. ((R)-PD)

A mixture of compound **1** (0.59 g, 1.4 mmol), compound **5** (2.1 g, 3.3 mmol) and tetrakis(triphenylphosphine)palladium(0) (100 mg, 0.08 mmol) in toluene (140 ml) was refluxed for 12 hours and cooled to room temperature. The reaction mixture was stirred with aqueous KF (10 wt%, 100 ml) for 30 minutes and extracted with toluene. The extract was dried over Na_2SO_4, filtered and concentrated in vacuo. The crude product was purified by a silica gel flash column chromatography (the eluant was hot cyclohexane : toluene = 2 : 1 and hot cyclohexane : THF = 1 : 5). The crude crystals were recrystallized from toluene several times to obtain (S)-**PD** as pale yellow crystals (0.19 g, 15 % in two steps).

^{1}H NMR (400MHz, $CDCl_3$) δ = 0.88 (6H, t, J = 6.8 Hz) , 1.30 (9H, d, J = 6.4 Hz) , 1.37 (4H, quint, J = 8.8 Hz) , 1.48 (3H, d, J = 6.0 Hz) , 1.66 (4H, quint, J = 7.6 Hz) , 2.39 (6H, s) , 4.13 (1H, dd, J = 4.4 Hz), 4.27 (1H, dd, J = 5.6 Hz), 4.75 (1H, sextet, J = 5.6 Hz) 6.67 (2H, d, J = 2.8 Hz), 6.96 (1H, t, J = 8.4 Hz) , 6.97 – 7.04 (8H, m) , 7.08 (1H, t, J = 8.4 Hz) , 7.22 – 7.31 (4H, m) IR (ATR) 792, 881, 958, 1002, 1128, 1227, 1299, 1302, 1370, 1459, 1508, 1629, 2851, 2928, 2964 cm^{-1}. Exact mass: 952.24. Molecular weight: 953.38. Mass (MALDI-TOF) Found: m/z (M^+): 952.26, 953.28, 954.28, 955.28, 956.28, 957.28. Calculated: m/z: 952.24, 953.24, 954.24, 954.25, 955.24, 956.24, 955.25, 956.23. Elemental analysis calcd (%): C, 66.77; H, 5.71; F, 3.99; O, 3.36; S, 20.18.; found: C, 66.7; H, 5.6.

Results and discussion

Phase transition behaviour of (S)-PD

(S)-**PD** exhibits a chiral nematic phase above room temperature, and forms a glassy chiral nematic phase in the supercooled state when the samples were cooled rapidly.

Figure 1 (a) shows DSC thermograms of (S)-**PD** on heating and cooling rates of 20 Kmin^{-1}. During the cooling process in the DSC thermograms, an exothermal peak (ΔH = 1.2 Jg^{-1}) was observed at 107 ºC. The small enthalpy is characteristic of isotropic-nematic or isotropic-chiral nematic phase transitions. Below the transition temperature, (S)-**PD** exhibited glass transition at 16 ºC. No exothermal peak originated from crystallization was observed. The asymmetric dimeric molecular structure should inhibit crystallization and promote the formation of the glassy state, in which the helical structure of a chiral nematic phase can be fixed. In the heating process, after a glass transition at 11 ºC, the sample crystallized at 54 ºC.

Between 102 ºC and 116 ºC, a different crystalline phase was observed, and it melted to change to the isotropic phase at 116 ºC. In a slower cooling rate (10 Kmin^{-1}), isotropic (S)-**PD** also exhibited monotropic chiral nematic phase, although it crystallized at 76 ºC as shown in Figure 1 (b). The large exothermal transition enthalpy (ΔH = 29.5 Jg^{-1}) indicates the phase below the transition temperature is not a smectic A, C, or C* phase. In the heating process, a crystal phase directly melted to change to the isotropic phase at 104 ºC.

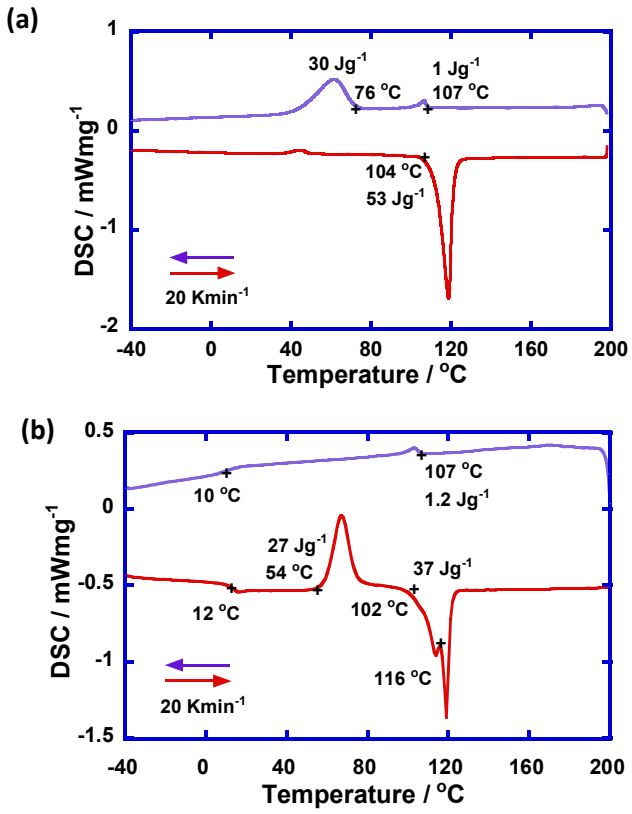

Figure 1 DSC thermograms of (S)-**PD** at heating and cooling rates of (a) 20 Kmin^{-1} and (b) 10 Kmin^{-1}.

Figure 2 shows an X-ray diffraction pattern of (S)-**PD** at room temperature. A broad halo around 2θ = 20 degree and no sharp peaks were appeared, which were characteristic of X-ray diffraction pattern in a chiral nematic phase. This halo is derived from liquid-like packing of alkyl chains. Around 2θ = 3 degree, a broad peak was observed and it is attributed to the short range order of the LC molecules in the chiral nematic phase. The spacing of the broad peak was 27 Å which corresponds to half of the molecular length of (S)-PD. A halo around 12 degree should be attributed to short range lateral order of the π-conjugated systems bearing a lateral substitutent.

In the chiral nematic phase of (S)-**PD**, a focal-conic texture was observed using a polarizing optical microscope as shown in Figure 3 (a). The birefringent domains were derived from the helical structures of (S)-**PD** with randomly oriented helical axes. After shearing stress was applied, the birefringent domains disappeared and oily streak texture was observed instead (Figure 3 (b)). This texture is typical of a chiral nematic phase in planer alignment in which the helical axes are perpendicular to the substrates. At 106 ˚C, the oily streak texture returned to the focal conic texture after DC voltage (>50V) was applied to the 9 μm-thick sample. Under a strong electric field, molecules tend to align parallel to the substrates, resulting in the change of the orientation of the helical axes because the molecule of (S)-**PD** has a strong permanent dipole moments perpendicular to the molecular axis due to the fluorinated benzene. Carrier transport properties of (S)-**PD** were examined in the states in which the helical axes are randomly oriented. (R)-**PD** exhibit the same optical textures as that of (S)-**PD** (see supporting information)

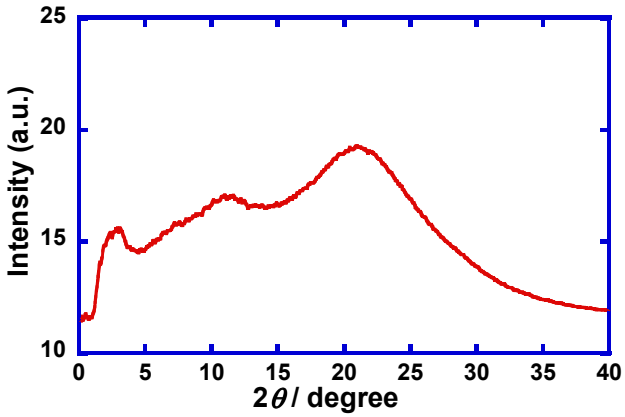

Figure 2 X-ray diffraction pattern of (S)-**PD** in a chiral nematic phase at room temperature.

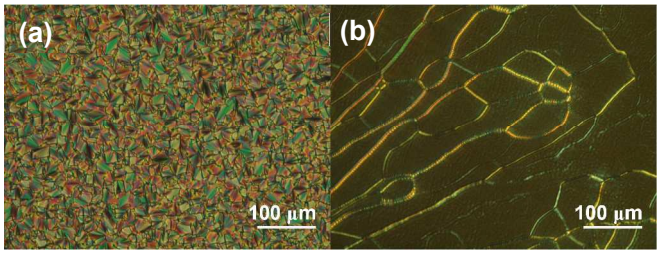

Figure 3 (a) Polarizing optical micrographs of (S)-**PD** at 106.0 ˚C during the cooling process, and (b) after applying shearing stress

Carrier transport property of (S)-PD

The TOF technique revealed that the dimeric compound (S)-**PD** exhibited efficient ambipolar electronic carrier transport property in the chiral nematic phase.

Without a DC bias, the helical axes were uniformly perpendicular to the substrate. Under the application of a DC bias, the uniformity of the orientation of the helical axes was broken and the helical axes oriented randomly. The optical texture changed to the state as shown in Figure 3(a). This change of the molecular alignment should be attributed to the strong dipole moment of C-F bonds of (S)-**PD**. During the measurement, the sample retained the chiral nematic phase without crystallization.

(b)

Figure 4 (a) shows transient photocurrents for positive carrier in the chiral nematic phase at 100 ºC. They are non-dispersive although they are influenced from space charges formed by photogenerated charge carriers. The mobility of the positive charge carrier was calculated to be 3.0×10^{-5} $cm^2V^{-1}s^{-1}$, which should be originated from electronic carrier transport process, but not from ionic one.

The carrier mobility in an ionic process is determined by the viscosity of the media and the ionic radius. Compared to the ionic transport in a typical nematic liquid crystal, 5CB (4-cyano-4'-pentylbiphenyl), (S)-**PD** has higher viscosity at 100 ºC than that of 5CB at room temperature. Assuming the movement of ionized LC molecules in the ionic processes, ionic radius of (S)-**PD** is larger than that of 5CB. This means that ionic mobility in the chiral nematic phase of (S)-**PD** at 100 ºC should be lower than that in the nematic phase of 5CB at room temperature. The positive carrier mobility in the nematic phase of 5CB is of the order of $10^{-6} \sim 10^{-5}$ $cm^2V^{-1}s^{-1}$. Therefore, the positive carrier in the chiral nematic phase of **(S)-PD** should be attributed to an electronic process, but not ionic one.

For negative carriers, the non-dispersive transient photocurrent curves were also observed in the chiral nematic phase as shown in Figure 4(b). The negative carrier mobility was 2.5×10^{-5} $cm^2V^{-1}s^{-1}$, which is comparable to that for holes. The negative charge carrier transport should also be attributed to an electronic process. The negative transient photocurrents disappeared in impure samples of (S)-**PD**, indicating the electronic nature of the negative charge carrier transport process.

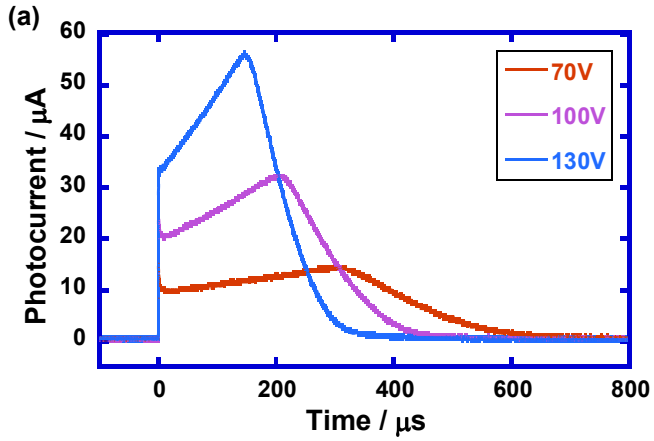

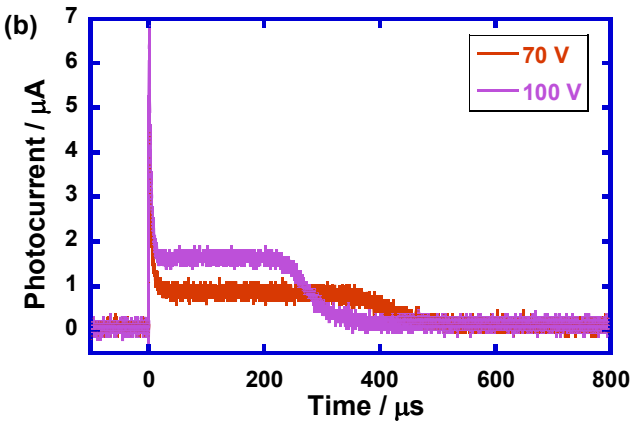

Figure 4 Transient photocurrent curves of (S)-**PD** for (a) positive and (b) negative charge carriers at 100 °C in the chiral nematic phase. Sample thickness is 9 μm.

In general, oligothiophene and polythiophene derivatives are p-type semiconductors because of their low ionization potentials. However, ambipolar electronic charge carrier transport has been observed in the bulk states of smectic phases of terthiophene and phenylterthiophene derivatives which are sufficiently purified.[3b,3g,4g] In field-effect transistors based on regioregular polythiophene, n-type operation was observed when dielectric layers without hydroxyl groups which capture electrons were used.[21]Figure 5 represents the temperature dependence of the hole and electron mobilities in the chiral nematic phase of (S)-**PD**. The carrier mobilities are field-independent. They increased monotonically with the temperature, indicating that the carrier transport process should be described by charge carrier hopping model, which is often applied to organic amorphous semiconductors.[22] However, this chiral nematic phase is fluidic and dynamic thermal fluctuation in the phase should influence on the carrier transport process. The effect of dynamic structural fluctuation on electronic charge carrier hopping processes has been pointed out in smectic and columnar phases.[3g,9e]

It should be noted that the hole and electron mobilities of (S)-**PD** are at least one order of magnitude higher than the hole mobility of the chiral nematic LCs bearing a binaphthyl group as a chiral part. That compound has phenylquaterthiophene moieties which include longer π-conjugated systems.[18b] However, the hole mobility was in the order of 10^{-6} $cm^2V^{-1}s^{-1}$ and field-dependent (see supporting information). It was plausible that the bulkiness of the electronically inactive chiral moiety inhibited the intermolecular electronic charge transfer, resulting in the low carrier mobility. Even though (S)-**PD** has shorter π-conjugated system (phenylterthiophene core), the carrier mobilities of the compound are five times higher than those of the compounds bearing bulky chiral moieties. The minimized volume of the chiral moiety of (S)-**PD** realized sufficient transfer intergral between the chromophores, resulting in the higher carrier mobility.

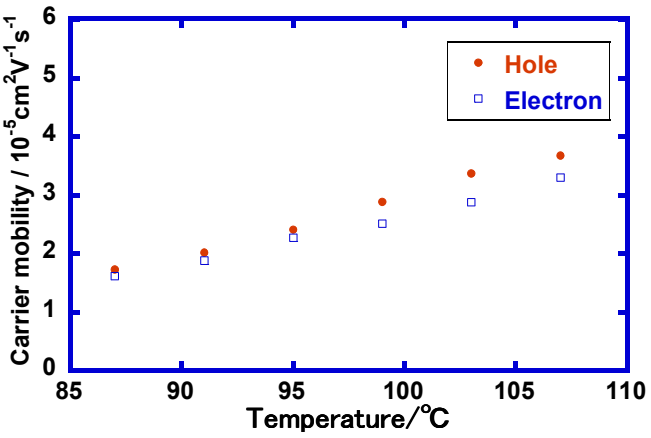

Figure 5 Hole (solid symbols) and electron (open symbols) mobilities of (S)-**PD** at 100 V as a function of the temperature.

Photonic band and circularly polarized photoluminescence spectra

Figure 6 shows transmission spectra of the mixtures of (S)-**PD** and R-form of the phenylterthiophene dimer ((R)-**PD**) which was synthesized in the same synthetic procedure as shown in Scheme 1. Below 460 nm, the transmittances of the samples were almost zero. This is attributed to the absorption band based on the electronic transition in the π-conjugated systems but not to reflection derived from the helical structures. The helical twisting power of (S)-**PD** is so strong that its stop band should be located in the UV region and the selective reflection was not observed in the wavelength region of visible light. By mixing (S)- and (R)-forms of the phenylterthiophene dimer, the wavelength area of the stop bands can be tuned between the near UV and infrared wavelength.

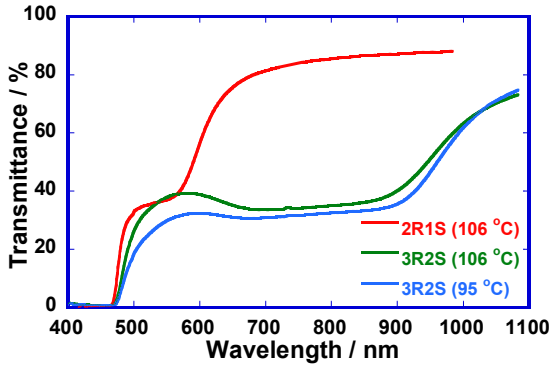

Figure 6 Transmittance spectra of (R)-**PD** / (S)-**PD** mixture at R : S = 2 :1 (2R1S) or 3 : 2 (3R2S) at 106 °C or 95 °C.

The (R) / (S) mixture at a ratio of 2 : 1 (**2R1S**) or 3 : 2 (**3R2S**) reflected green or red light at 106 ºC, respectively. Mixture **3R2S** had the wide range stop band width over 200 nm, attributed to large anisotropy in refractive index due to the extended ***π***-conjugated system and a high order parameter. The stop band was slightly red-shifted by decreasing the temperature from 106 ºC to 95 ºC, and strong absorption of the chromophore was observed below 460 nm from the transmittance spectra. Compared with mixture **3R2S**, mixture **2R1S** exhibited the shorter stop band width of approximately 100 nm.

The stop band width $\Delta\lambda$ is defined as equation 2, where Δn is the birefringence and n is the refractive index at the central wavelength λ of the stop band.

$$\Delta\lambda = \lambda \cdot \frac{\Delta n}{n} \qquad (2)$$

Mixture **2R1S** has the shorter central wavelength than that of mixture **3R2S**, resulting in the narrow stop band width.

Sample **2R1S** exhibited the stop band between 480 nm and 580 nm, which overlap with the photoluminescence spectrum of phenylterthiophene core of (S)- and (R)-**PD**. CPL with opposite handedness to that of the helix of the chiral nematic phase is suppressed within the stop band whereas CPL with the same handedness is emitted. Figure 7 represents left- and right-handed circularly polarized photoluminescence spectra from sample **2R1S**. The left-handed CPL from 500 nm to 550 nm was strongly quenched in sample **2R1S**. From this sample, right handed CPL luminescence was emitted and the helical structure of the chiral nematic phase of the sample was left-handed.

The circular dissymmetry factor g_e is defined as equation 3, where I_L and I_R are intensities of left- and right-handed circularly polarized light, respectively.

$$g_e = \frac{2(I_L - I_R)}{(I_L + I_R)} \qquad (3)$$

Sample **2R1S** quenched left-handed CPL and emitted right-handed CPL with the g_e value up to 1.2 and 1.5 for 5 μm- and 9 μm-thick samples, respectively.

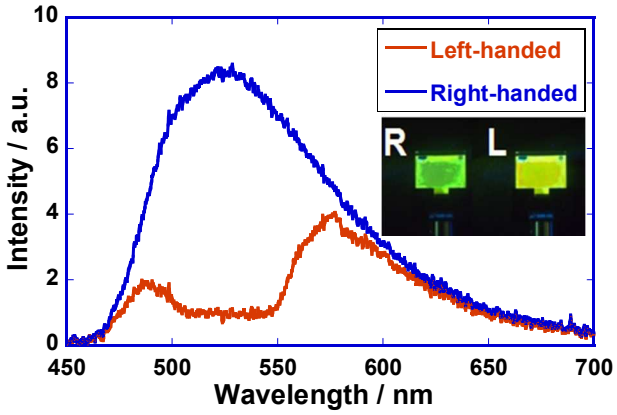

Figure 7 Circularly polarized photoluminescence spectra from 9 μm-thick chiral nematic thin film of (R)-**PD** / (S)-**PD** mixture **2R1S** at 106 °C. The inset indicates photographs of the fluorescent LC cell through circularly polarized filters consisting of $\lambda/2$ and $\lambda/4$ plates, which transmits right-handed CPL. The wavelength of the excitation light is 360 nm.

The inset indicates photographs of the LC cell filled with the mixture of **2R1S** at 106 ºC. In the left photograph, right-handed CPL is observed through a circularly polarized filter

and the colour of the fluorescence is green. In the right photograph, the colour is yellow because the left-handed circularly polarized green light emission is suppressed in the helical structure in the chiral nematic phase.

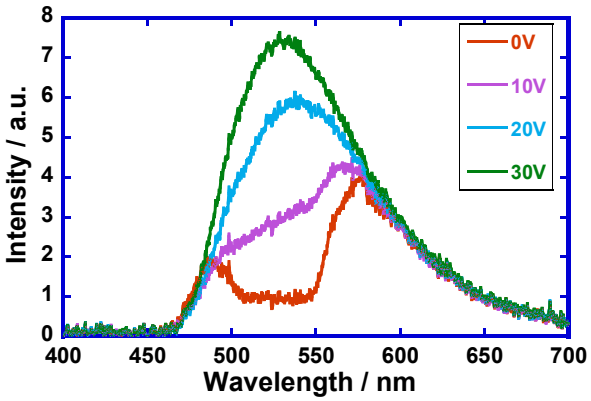

Figure 8 Photoluminescence spectra from a mixture **2R1S** at 106 °Cthrough a circularly polarized filter transmitting right-handed CPL under the application of DC voltage. The sample thickness is 9 μm. The wavelength of the excitation light is 360 nm.

In the fluidic chiral nematic phase, CPL fluorescence can be tuned by the application of a DC voltage. Figure 8 shows photoluminescence spectra from a mixture **2R1S** at 106 ºC through a circularly polarized filter transmitting right-handed CPL under the application of DC voltage. Without the DC voltage, the LC molecules align parallel to the surface of the substrates and the helical axis is perpendicular to the substrate. Increasing the applied voltage, the direction of the helical axes is disordered and the polarization of the fluorescence is lost. When the DC voltage is turned off, the polarization of the fluorescence is recovered. This result indicates that the colour of the fluorescence can also be tuned between green and yellow by the application of DC voltage. The response time is in the order of several hundred ms.

Comparison with other systems

Compared to conventional non-LC organic or inorganic CPL emitting materials, mixture **2R1S** exhibited higher quality CPL emission. Chiral metal complexes and chiral conjugated polymers, which are typical CPL emissive materials, exhibited very low g_e values: 0.47[23a] and 0.2[23b], respectively. Achiral conjugated polymers emitted CPL with g_e value of 0.5 by blended with chiral small molecules,[23c] and inorganic semiconductors were reported as CPL emitters although the g_e values are 0.4 ~ 0.9.[23d-e] Chiral cyclophane derivatives were recently reported and the g_e values were in the order of 10^{-2}. In our result, the obtained g_e value is 1.5 and larger than those of the previous studies.[23f]

Chen and co-workers studied glass-forming or polymerizable chiral nematic LCs containing fluorescent dyes have been studied.[14c] Fluorescent conjugated polymers forming chiral nematic LC thin films have also been investigated. However, the g_e value were low.

The g_e value obtained in this study is higher than those observed in chiral nematic conjugated polymers and is comparable to that in the chiral nematic phase of dimeric LC consisting of two phenylquaterthiophene and one binaphthyl moieties. The g_e value obtained in this study is slightly lower than that in the chiral nematic phase of bisphenylthenylfluorene derivatives, in which high quality CPL emission was obtained in the wavelength region over 100 nm.

Terthiophene dimer (S)/(R)-**PD** in this study has an advantage in the carrier transport characteristics over the chiral nematic LCs reported previously. (S)/(R)-**PD** exhibited non-dispersive ambipolar carrier transports with the mobilities of the order of 10^{-5} $cm^2V^{-1}s^{-1}$. Binaphthyl derivatives bearing phenylquaterthiophene parts exhibited one magnitude lower hole mobility of the order of 10^{-6} $cm^2V^{-1}s^{-1}$ in a chiral nematic phase (see supporting information). The bisphenylthenylfluorene derivative to emit high quality CPL[18a] exhibits higher hole mobility of the order of 10^{-4} $cm^2V^{-1}s^{-1}$ at room temperature, but electron transport was not reported. Only a few papers reported high carrier mobility of the order of 10^{-4} $cm^2V^{-1}s^{-1}$ in a chiral nematic phase.[17a] However, these compounds did not exhibit a glass transition or ambipolar carrier transport,[17b-e] which are both significant properties for electrically pumped CPL emitting devices.

In the fluidic chiral nematic phase, reversible conversion between circularly polarized and non-polarized states in the photoluminescence by the application of DC bias is possible. As a consequence, the emission colour is also electrically switched between green and yellow.

Moreover, (S)-**PD** has an unusually short helical pitch, whereas most of chiral nematic LCs have stop band in visible or infrared area. Therefore, the reflection band can be tuned in the blue and near infrared wavelength by mixing the enantiomers or changing the temperature. The short helical pitch of (S)-**PD** also means that it can act as a chiral dye dopant for conventional nematic LC and applied to luminescent systems to emit CPL. We already observed that 2.6 mol% of (S)-**PD** doped 5CB showed selective reflection in visible light wavelength area. The investigation of the properties of (S)-**PD** as a chiral dye dopant is in progress.

In conventional electroluminescence devices, thin active layers with the thickness of several ten nm are used because a minimized DC voltage form a sufficiently strong electric field to inject holes and electrons from the electrodes and to transport them. In the chiral nematic phase, helical pitch is much larger than the standard thickness of the active layers. For the construction of electrically pumped chiral nematic systems, it is

indispensable to realize efficient carrier injection and transport under a weaker electric field.

Conclusions

In conclusion, we synthesized chiral dimer (S)- **PD** bearing two phenylterthiophene parts linked by a single chiral (S)-propane moiety. The chiral dimers form fluidic helical superstructures, which can be fixed in the supercooled state around room temperature. The phenylterthiophene core can also act as a hopping site of charge carriers. (S)-**PD** exhibited efficient ambipolar electronic carrier transport properties in the helicity. Because of the minimized chiral moiety, the hole and electron mobilities are of the order of 10^{-5} $cm^2V^{-1}s^{-1}$, which is higher than that of conventional chiral nematic LCs bearing a bulky chiral moiety. (S)-**PD** mixed with its enantiomer emitted circularly polarized light with the g_e value of 1.5. In the fluidic chiral nematic phase, the circularly polarized photoluminescence can be changed to non-polarized photoluminescence by the application of DC voltage reversibly. The colour of the luminescence is also switched between green and yellow by the electric field. The helical pitch is unusually short and besides (S)-**PD** bears phenylterthiphene chromophore. Therefore, (S)-**PD** has a possibility to act as a chiral dye dopant for conventional nematic LCs and applied to luminescent systems to emit CPL.

Acknowledgements

This study was financially supported by the Japan Security Scholarship Foundation, the Ogasawara Foundation, a Grant-in-Aid for Scientific Research on Innovative Areas (Coordination Programming, no. 24108729 and Element-Block Polymers, no. 25102533) from the Ministry of Education, Culture, Sports, Science and Technology (MEXT), a Grant-in-Aid for Scientific Research (B) (no. 22350080) from the Japan Society for the Promotion of Science (JSPS), the Iwatani Naoji Foundation, the Asahi Glass Foundation, the Murata Science Foundation, and the TEPCO Memorial Foundation. The authors thank Dr. A. Sonoda at Health Research Institute, National Institute of Advanced Industrial Science and Technology for help with the NMR measurement. The authors also thank Prof. T. Ishii and Prof. T. Kusunose at Kagawa University for help with the X-ray diffraction and the DSC measurements. The elemental analyses were carried out in the Engineering Research Equipment Centre of Kumamoto University and Sumika Chemical Analysis Service Ltd. Polyimide solution was supplied by Nissan Chemical Industry, Ltd.

Notes and references

Department of Advanced Materials Science, Faculty of Engineering, Kagawa University, 2217-20 Hayashi-cho, Takamatsu, Kagawa 761-0396 Japan. Fax: (+81)-87-864-2411; Tel: (+81)-87-864-2411; E-mail: m-funa@eng.kagawa-u.ac.jp

1 (a) W. Pisula, M. Zorn, J. Y. Chang, K. Müllen, R. Zentel, *Macromol. Rapid Commun*., 2009, **30**, 1179-1202. (b) Y. Shimizu, K. Oikawa, K. Nakayama, D. Guillon, *J. Mater. Chem*. 2007, **17**, 4223-4229. (c) M. O'Neill, S. M. Kelly, *Adv. Mater*., 2011, **23**, 566-584. (d) M. Funahashi, H. Shimura, M. Yoshio, T. Kato, *Structure and Bonding*, 2008, **128**, 151-179. (e) M. Funahashi, T. Yasuda, T. Kato, *Handbook of Liquid Crystals* 2nd Ed. Wiley-VCH, 2014, **8**, 675-708.

2 (a) D. Adam, F. Closs, T. Frey, D. Funhoff, D. Haarer, H. Ringsdorf, P. Schuhmacher, K. Siemensmeyer, *Phys. Rev. Lett*., 1993, **70**, 457-460. (b) N. Boden, R. J. Bushby, J. Clements, B. Movaghar, K. J. Donovan, T. Kreouzis, *Phys. Rev. B*, 1995, **52**, 13274-13280. (c) A. M. van de Craats, J. M. Warman, A. Fechtenkötter, J. D. Brand, M. A. Harbison, K. Müllen, *Adv. Mater*., 1999, **11**, 1469-1472. (d) M. Ichihara, A. Suzuki, K. Hatsusaka, K. Ohta, *Liq. Cryst*., 2007, **34**, 555-567. (e) K. Ban, K. Nishikawa, K. Ohta, A. M. van de Craats, J. M. Warman, I. Yamamoto, H. Shirai, *J. Mater. Chem*., 2001, **11**, 321-331. (f) A. Demenev, S. H. Eichhorn, T. Taerum, D. Perepichka, S. Patwardhan, F. C. Grozema, L. D. A. Siebbeles, *Chem. Mater*., 2010, **22**, 1420-1428. (g) J. Simmerer, B. Glüsen, W. Paulus, A. Kettner, P. Schuhmacher, D. Adam, K.-H. Etzbach, K. Siemensmeyer, J. H. Wendorf, H. Ringsdorf, D. Haarer, *Adv. Mater*., 1996, **8**, 815-819.

3 (a) M. Funahashi, J. Hanna, *Phys. Rev. Lett*., 1997, **78**, 2184-2187. (b) M. Funahashi, J. Hanna, *Appl. Phys. Lett*., 2000, **76**, 2574-2576. (c) M. Funahashi, J. Hanna, *Adv. Mater*., 2005, **17**, 594-598. (d) K. Oikawa, H. Monobe, J. Takahashi, K. Tsuchiya, B. Heinrich, D. Guillon, Y. Shimizu, *Chem. Commun*., 2005, 5337-5339. (e) A. Matsui, M. Funahashi, T. Tsuji, T. Kato, *Chem. Eur. J*., 2010, **16**, 13465-13472. (f) H. Aboubakr, M.-G. Tamba, A. K. Diallo, C. Videlot-Ackermann, L. Belec, O. Siri, J.-M. Raimundo, G. H. Mehl, H. Brisset, *J. Mater. Chem*., 2012, **22**, 23159-23168. (g) M. Funahashi, F. Zhang, N. Tamaoki, J. Hanna, *ChemPhysChem*, 2008, **9**, 1465-1473. (h) M. Funahashi, T. Ishii, A. Sonoda, *ChemPhysChem*, 2013, **14**, 2750-2758.

4 (a) A. J. J. M. van Breemen, P. T. Herwig, C. H. T. Chlon, J. Sweelssen, H. F. M. Schoo, S. Setayesh, W. M. Hardeman, C. A. Martin, D. M. de Leeuw, J. J. P. Valeton, C. W. M. Bastiaansen, D. J. Broer, A. R. Popa-Merticaru, S. C. J. Meskers, *J. Am. Chem. Soc*., 2006, **128**, 2336-2345. (b) M. Funahashi, F. Zhang, N. Tamaoki, *Adv. Mater*., 2007, **19**, 353-358. (c) W. Pisula, A. Menon, M. Stepputat, I. Lieberwirth, U. Kolb, A. Tracz, H. Sirringhaus, T. Pakula, K. Müllen, *Adv. Mater*., 2005, **17**, 684-689. (d) M. Funahashi, *Polym. J*., 2009, **41**, 459-469. (e) F. Zhang, M. Funahashi, N. Tamaoki, *Org. Electr*., 2010, **11**, 363-368.

5 (a) T. Hassheider, S. A. Benning, H.-S. Kitzerow, M.-F. Achard, H. Bock, *Angew. Chem., Int. Ed*., 2001, **40**, 2060-2063. (b) M. P. Aldred, A. E. A. Contoret, S. R. Farrar, S. M. Kelly, D. Mathieson, M. O'Neill, W. C. Tsoi, P. Vlachos, *Adv. Mater*., 2005, **17**, 1368-1372. (c) S. A. Benning, R. Oesterhaus, H.-S. Kitzerow, *Liq. Cryst*., 2004, **31**, 201-205. (d) M. W. Lauhof, S. A. Benning, H.-S. Kitzerow, V. Vill, F. Scheliga, E. Thorn-Csányi, *Synth. Met*., 2007, **157**, 222-227.

6 (a) T. Hori, Y. Miyake, N. Yamasaki, H. Yoshida, A. Fujii, Y. Shimizu, M. Ozaki, *Appl. Phys. Exp*., 2010, **3**, 101602. (b) W. Shin, T. Yasuda, G. Watanabe, Y. S. Yang, C. Adachi, *Chem. Mater*., 2013, **25**, 2549-2556.

7 M. Funahashi, *J. Mater. Chem. C*, 2014, **2**, 7451-7459.

8 (a) T. Kato, T. Yasuda, Y. Kamikawa, M. Yoshio, *Chem. Commun*., 2009, 729-739; (b) T. Yasuda, H. Ooi, J. Morita, Y. Akama, K. Minoura, M. Funahashi, T. Shimomura, T. Kato, *Adv. Funct. Mater*., 2009, **19**, 411-419; (c) M. Yoneya, *Chem. Rec*., 2011, **11**, 66-76; (d) S. Yazaki, M. Funahashi, T. Kato, *J. Am. Chem. Soc*., 2008, **130**, 13206-13207; (e) S. Yazaki, M. Funahashi, J. Kagimoto, H. Ohno, T. Kato, *J. Am. Chem. Soc*., 2010, **132**, 7702-7708.

9 (a) M. Funahashi, A. Sonoda, *Org. Electr*., 2012, **13**, 1633-1640; (b) M. Funahashi, A. Sonoda, *J. Mater. Chem*., 2012, **22**, 25190-25197; (c) M. Funahashi, A. Sonoda, *Dalton Trans*., 2013, **42**, 15987-15994; (d) M. Funahashi, M. Yamaoka, K. Takenami, A. Sonoda, *J. Mater. Chem. C*, 2013, **1**, 7872-7878; (e) M. Funahashi, T. Ishii, A. Sonoda, *Phys. Chem. Chem. Phys*., 2014, **16**, 7754-7763.

10 (a) N. Tamaoki, A. V. Parfenov, A. Masaki, H. Matsuda, *Adv. Mater*. 1997, **9**, 1102-1104. (b) V. A. Mallia, N. Tamoaki, *Chem. Soc. Rev*., 2004, **33**, 76-84 (c) N. Tamaoki, *Adv. Mater*., 2001, **13**, 1135-1147; (d) Y. Kim, M. Wada, N. Tamaoki, *J. Mater. Chem. C*, 2014, **2**, 1921-1926; (e) K. Akagi, *Chem. Rev*., 2009, **109**, 5354–5401; (f) C. T. Imirie, *Struct. Bond*., 1999, **95**, 149-192.

11 (a) K. Kogo, H. Maeda, H. Kato, M. Funahashi, J. Hanna, *Appl. Phys. Lett*., 1999, **75**, 3348-3350. (b) Y. Funatsu, A. Sonoda, M. Funahashi, *Trans. Mater. Res. Soc. Jpn*., 2013, **38**, 373-375. (c) Y. Funatsu, A. Sonoda, M. Funahashi, *J. Mater. Chem. C*, 2015, **3** in press.

12 (a) K. J. Ihn, J. A. N. Zasadzinski R. Pindak, A. J. Slaney, J. Goodby, *Science*, 1992, **258**, 275-278; (b) J. Fernsler, L. Hough, R.-F. Shao, J. E. Maclennan, L. Navailles, M. Brunet, N. V. Madhusudana, O. Mondain-Monval, C. Boyer, J. Zasadzinski, J. A. Rego, D. M. Walba, N. A. Clark, *Proc. Nat. Acad. Sci*., 2005, **102**, 14191–14196.

13 (a) H. Kikuchi, M. Yokota, Y. Hisakado, H. Yang, T. Kajiyama, *Nature Materials*, 2002, **1**, 64-68; (b) H. S. Kitzerow, H. Schmid, A. Ranft, G. Heppke, R. A. M. Hikmet, J. Lub, *Liq. Cryst*., 1993, **14**, 911-916.

14 (a) D. Katsis, D. U. Kim, H. P. Chen, L. J. Rothberg, S. H. Chen, T. Tsutsui, *Chem. Mater*. 2001, **13**, 643-647; (b) S. H. Chen, D. Katsis, A. W. Schmid, J. C. Mastrangelo, T. Tsutsuik, T. N. Blanton, *Nature*, 1999, **397**, 506-508; (c) Y. Geng, A. Trajkovska, S. W. Culligan, J. J. Ou, H. M. P. Chen, D. Katsis, S. H. Chen, *J. Am. Chem. Soc*., 2003, **125**, 14032-14038; (d) K. Watanabe, I. Osaka, S. Yorozuya, K. Akagi, *Chem. Mater*. 2012, **24**, 1011−1024; (e) Y. Nagata, K. Takagi, M. Suginome, *J. Am. Chem. Soc*., 2014, **136**, 9858−9861; (f) A.Yu. Bobrovsky, N.I. Boiko, V.P. Shibaev and J.H. Wendorff, *Adv. Mater*., 2003, 15, 282-287;

15 (a) L.-W. Li, L.-G. Deng, *Eur. Phys. J. B*, 2013, **86**, 112; (b) S. Furumi, N. Tamaoki, *Adv. Mater*., 2010, **22**, 886–891; (c) A. Chanishvili, G. Chilaya, G. Petriashvili, R. Barberi, R. Bartolino, G. Cipparrone, A. Mazzulla, L. Oriol, *Adv, Mater*., 2004, **16**, 791–795; (d) M. Ozaki, M. Kasano, T. Kitasho, D. Ganzke, W. Haase, K. Yoshino, *Adv. Mater*., 2003, **12**, 974–977; H. Finkelmann, S. T. Kim, A. Munoz, P. Palffy-Muhoray, B. Taheri, *Adv. Mater*., 2001, **14**, 1069-1072; (e) F. Araoka, K.-C. Shin, Y. Takanishi, K. Ishikawa, H. Takezoe, Z. Zhu, and T. M. Swager, *J. Appl. Phys*. 2003, **94**, 79-283.

16 (a) K. Yoshino, K. Yamashiro, and Y. Inuishi, *Jpn. J. Appl. Phys*., 1974, **13**, 1471-1472; (b) Y. Shimizu, K. Shigeta, S. Kusabayashi, *Mol. Cryst. Liq. Cryst*., 1986, **140**, 105-117; (c) S. Murakami, H. Naito, M. Okuda, A. Sugimura, *J. Appl. Phys*., 1995, **78**, 4533-4537; (d) A. Sawada, S. Naemura, *Jpn J. Appl. Phys*., 2002, **41**, L195-197.

17 (a) S. R. Farrar, A. E. A. Contoret, M. O'Neill, J. E. Nicholls, G. J. Richards, S. M. Kelly, *Phys. Rev. B*, 2002, **66**, 125107; (b) K. L. Woon, M. P. Aldred, P. Vlachos, G. H. Mehl, T. Stirner, S. M. Kelly, M. O'Neill, *Chem. Mater*., 2006, **18**, 2311-2317; (c) M. Funahashi, N. Tamaoki, *ChemPhysChem*, 2006, **7**, 1193-1197; (d) M. Funahashi, N. Tamaoki, *Chem. Mater*., 2007, **19**, 608-617; (e) M. Nuita, J. Sakuda, Y. Hirai, M. Funahashi, T. Kato, *Chem. Lett*., 2011, **40**, 412-413; (f) K. Tokunaga, Y. Takayashiki, H. Iino, J. Hanna, *Phys. Rev. B*, 2009, **79**, 033201.

18 (a) K. L. Woon, M. O'Neill, G. J. Richards, M. P. Aldred, S.M. Kelly, A.M. Fox, *Adv. Mater*., 2003, **15**, 1555-1558; (b) M. Funahashi, N. Tamaoki, *Mol. Cryst. Liq. Cryst*., 2007, **475**, 123-135.

19 (a) R. G. Kepler, *Phys. Rev*., 1960, **119**, 1226-1229; (b) W. E. Spear, *J. Non-Cryst. Solid*, 1968, **1**, 197-214.

20 J. K. Stille, Angew. Chem. Int. Ed. Engl., 1986, 25, 508-524.

21 L.-L. Chua, J. Zaumseil, J.-F. Chang, E. C.-W. Ou, P. K.-H. Ho, H. Sirringhaus, R. H. Friend, *Nature*, 2005, **434**, 194-199.

22 (a) H. Bässler, *Phys. Status Solidi B*, 1993, **175**, 15-56. (b) M. van der Auweraer, F. C. Schryver, P. M. Borsenberger, H. Bässler, *Adv. Mater*., 1994, **6**, 199-213. (c) A. Köhler, H. Bässler, *Top. Curr. Chem*., 2012, **312**, 1-66. (d) R. Goehoorn, P. A. Bobbert, *Phys. Status Solidi A*, 2012, **209**, 2354-2377. (e) T. Nagase, K. Kishimoto, H. Naito, *J. Appl. Phys*., 1999, **86**, 5026-5035.

23 (a) T. Harada, Y. Nakano, M. Fujiki, M. Naito, T. Kawai, Y. Hasegawa, *Inorg. Chem*., 2009, **48**, 11242–11250; (b) M. Oda, H.-G. Nothofer, G. Lieser, U. Scherf, S. C. J. Meskers, D. Neher, *Adv. Mater*. 2000, **12**, 362-365; (b) Y. Yang, R. C. da Costa, D.-M. Smilgies, A. J. Campbell, M. J. Fuchter, *Adv. Mater*., 2013, **25**, 2624–2628; (c) Y. Yang, R. Correa da Costa, D.-M. Smilgies, A. J. Campbell, M. J. Fuchter, *Adv. Mater*., 2013, **25**, 2624–2628; (d) K. Konishi, M. Nomura, N. Kumagai, S. Iwamoto, Y. Arakawa, M. Kuwata-Gonokami, *Phys. Rev. Lett*., 2011, **106**, 057402; (e) Y. J. Zhang, T. Oka, R. Suzuki, J. T. Ye, Y. Iwasa, *Science*, 2014, **16**, 725-728; (d) S. M. Jeong, Y. Ohtsuka, N. Y. Ha, Y. Takanishi, K. Ishikawa, H. Takezoe, S. Nishimura, G. Suzaki, *Appl. Phys. Lett*., 2007, **90**, 211106; (e) E. Peeters, M. P. T. Christiaans, R. A. J. Janssen, H. F. M. Schoo, H. P. J. M. Dekkers, E. W. Meijer, *J. Am. Chem. Soc*. 1997, **119**, 9909-9910; (f) Y. Morisaki, M. Gon, T. Sasamori, N. Tokito, Y. Chujo, *J. Am. Chem. Soc*., 2014, **136**, 3350-3353.

Table of Contents

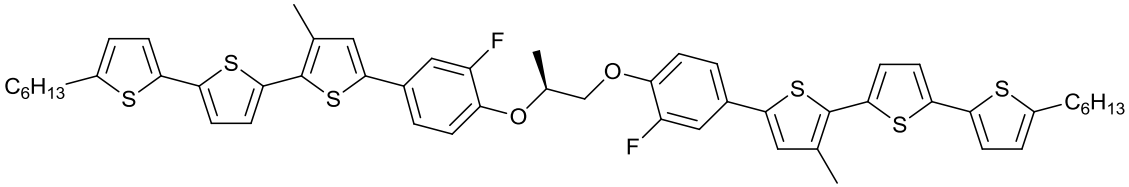

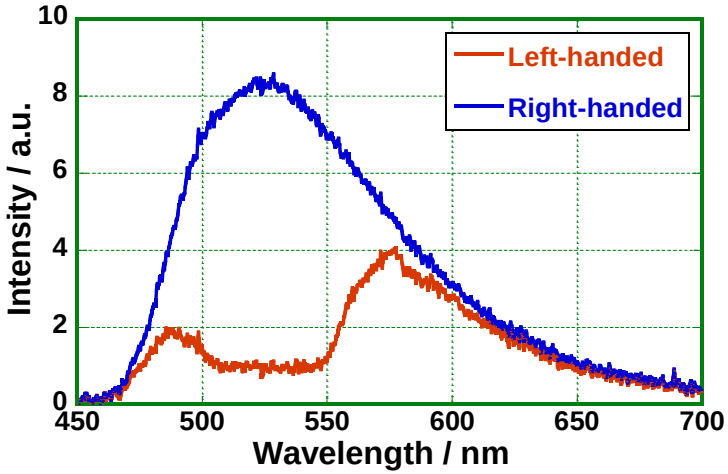

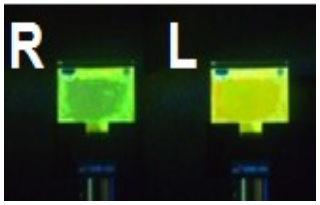

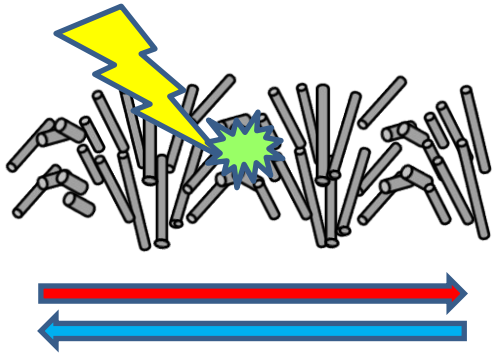

Circularly polarized fluorescence

Ambipolar carrier transport